

Crystalline electric fields and the magnetic ground state of the novel Heusler intermetallic YbRh_2Pb

D. A. Sokolov^{1,†}, M. S. Kim¹, M. C. Aronson^{1,3}, C. Henderson², and P. W. Stephens³

¹⁾ *Department of Physics, The University of Michigan,
Ann Arbor, Michigan 48109-1120, USA*

²⁾ *Department of Geological Sciences,
The University of Michigan,
Ann Arbor, Michigan 48109-1120, USA
and*

³⁾ *Department of Physics and Astronomy,
State University of New York,
Stony Brook, New York 11794, USA*

We have synthesized a new intermetallic compound with a distorted Heusler structure, YbRh_2Pb . We present a study of the magnetic, thermal, and transport properties. Heat capacity measurements revealed that YbRh_2Pb orders magnetically below $T_N=0.57$ K from a paramagnetic state with substantial crystal electric field splitting. Magnetic field further splits the ground state, which leads to the suppression of magnetic order in YbRh_2Pb .

PACS numbers: 71.20.Eh, 75.40.Cx

I. INTRODUCTION

Analysis of the magnetic properties of compounds containing rare-earths is complicated when the Kondo temperature and crystalline electric field (CEF) splitting of the ground state are comparable to the ordering temperature. The CEF reduces the degeneracy of the total angular momentum J , often leading to deviations from the Curie-Weiss behavior of the temperature dependent magnetic susceptibility. The CEF scheme in high symmetry crystal structures can be established using heat capacity and magnetic susceptibility measurements, making it straightforward in this case to isolate possible Kondo effects as well as phenomena related to the magnetic ordering. The Heusler compounds are an especially attractive class of materials in which to pursue such studies, as they contain a cubic lattice of rare-earth ions¹. Rare-earth based Heusler compounds generally order antiferromagnetically at low temperatures due to the conduction electron mediated Ruderman-Kittel-Kasuya-Yosida (RKKY) interaction among well-localized rare earth moments^{2,3,4,5,6,7,8,9,10}. Intriguingly, coexistence of antiferromagnetism and superconductivity has been reported for some of these compounds^{2,4,5,7,8,9}. In this article we report a new Yb based tetragonally distorted Heusler compound, YbRh_2Pb , with a magnetic ordering temperature comparable to the splitting in the ground state manifold. The tetragonal distortion of the cubic Heusler structures was reported previously and was attributed to an electronic instability of the band Jahn-Teller type¹¹. We demonstrate that the degeneracy of the manifold in YbRh_2Pb is partially lifted by both the CEF and the magnetic field. The magnetism of YbRh_2Pb , characterized by total angular momentum, J , is suppressed by the reduced degeneracy of the ground state.

II. EXPERIMENTAL DETAILS

Samples of YbRh_2Pb were grown from Pb flux. They had the appearance of faceted cubes with typical dimensions of 2 mm. The grains were etched to remove excess Pb using a 1:1 solution of H_2O_2 and acetic acid. A small amount of one grain was crushed, and a powder X-ray diffraction pattern was collected at room temperature. A Si(111) double crystal monochromator selected a beam of $0.70050(2)$ Å X-rays at the X16C beamline of the National Synchrotron Light Source at Brookhaven National Laboratory. The diffracted X-rays were analyzed by a Ge(111) crystal and detected with a NaI scintillation counter. The sample, on a quartz zero-background holder, was oscillated 2 degrees at each point during data collection. Microanalysis measurements were performed on a CAMECA SX100 electron microprobe at the University of Michigan. Electron beam voltage was 20 keV, beam current was 10 nA, and the Yb $L\alpha$, Rh $L\alpha$, and Pb $M\alpha$ X-ray intensities were calibrated from synthetic YbPO_4 , synthetic CeRhSn , and natural PbS standards respectively. Matrix elements were calculated using CAMECA PAP data reduction routine. The magnetic susceptibility was measured using a Quantum Design SQUID magnetometer at temperatures from 1.8 K to 300 K. Measurements of the electrical resistivity and heat capacity were performed using a Quantum Design Physical Property Measurement System at temperatures from 0.35 K to 300 K and in magnetic fields up to 4 T.

III. RESULTS AND DISCUSSION

Electron microprobe experiments found that the stoichiometry was uniform over the surface of the sam-

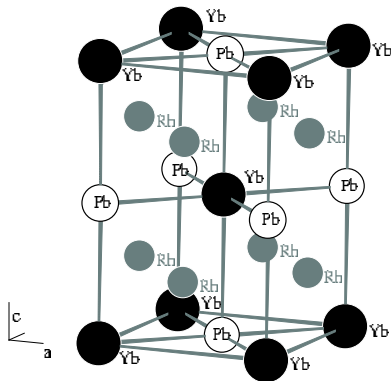


FIG. 1: Crystal structure of YbRh_2Pb . Rh atoms occupy $(0,1/2,1/4)$ sites, Yb atoms are at $(0,0,0)$ and Pb atoms are at $(0,0,1/2)$ positions.

ples, with the elemental ratios for Yb:Rh:Pb of $1 \pm 0.02 : 2 \pm 0.04 : 1 \pm 0.02$. Examination of several small grains chipped from the faceted as-grown samples with a Bruker Smart CCD X-ray diffractometer revealed that they were multiply twinned. The powder X-ray diffraction pattern was indexed and refined using Topas software¹². The powder X-ray diffraction pattern showed the presence of Pb and several other weak unidentified peaks. The unit cell was found to be tetragonal, with dimensions $a=4.5235(4)\text{\AA}$, $c=6.9864(6)\text{\AA}$, probable space group $I4/mmm$. The small, high symmetry unit cell suggested a distorted Heusler alloy structure, and indeed a satisfactory refinement was found with Yb at $(0,0,0)$, Pb at $(0,0,1/2)$, Rh at $(0,1/2,1/4)$. Refinement of occupancies showed no significant (less than 5%) mixing of atoms in the various sites. The crystal structure of YbRh_2Pb is shown in Fig. 1. The observation of cube-shaped grains containing multiple twins suggested that the sample material was a cubic phase when it solidified from the melt, and transformed into the tetragonal phase as it cooled. Similar behavior in Heusler intermetallic phases has been noted previously, and ascribed to an electronic band-driven Jahn-Teller distortion¹¹.

The electrical resistivity ρ was measured from 0.35 K to 300 K. As shown in Fig. 2, the resistivity is that of a good metal, decreasing from the value of $16 \mu\Omega\cdot\text{cm}$ at 300 K to $2 \mu\Omega\cdot\text{cm}$ at the lowest temperature. The inset to Fig. 2 shows a partial superconducting transition at $T_c=7.2$ K due to residual Pb flux, followed by another partial superconducting transition at $T_c=3$ K, which we believe is due to trace amounts of superconducting RhPb_2 ¹³. We performed Meissner effect measurements which confirmed these conclusions, finding a volume fraction of less than 1% for the proposed Pb inclusions, and an even smaller volume fraction for RhPb_2 . The almost linear temperature dependence of $\rho(T)$ demonstrated in Fig. 2 for temperatures above ~ 70 K is remarkable. While this linearity is manifestly not that of a normal Fermi liquid ground state, it may indicate that the resistivity is derived from the electron-phonon interaction and further that the De-

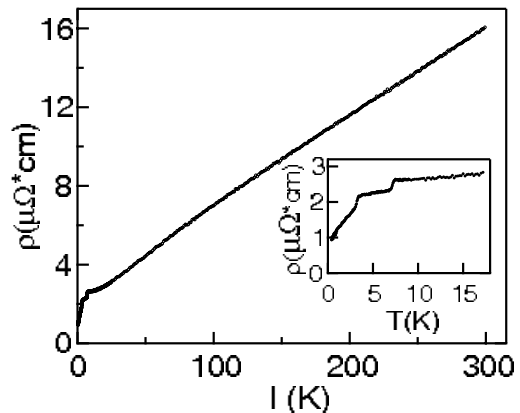


FIG. 2: Temperature dependence of the electrical resistivity of YbRh_2Pb measured in zero field. Inset: Expanded view of low temperatures, showing two partial superconducting transitions at 7.2 K and 3 K due to trace amounts of Pb and RhPb_2 , respectively.

bye temperature in YbRh_2Pb is unusually small. However, we later show, using the heat capacity data that the Debye temperature in YbRh_2Pb is ~ 213 K. It is notable as well that the resistivity does not saturate at high temperatures, suggesting that the electronic mean free path is still much larger than the lattice constant at room temperature. We cannot entirely rule out the possibility that the fundamental electronic excitations are themselves anomalous, as was found in the normal state of the high temperature oxide superconductors.¹⁴

The magnetic properties of YbRh_2Pb establish that the Yb^{3+} moments are well localized. The temperature dependence of the dc magnetic susceptibility $\chi(T)$ was measured in a field of 1000 Oe. The data are plotted as $1/\chi(T)$ as a function of temperature in Fig. 3. These data are only linear between 100 K and 300 K, where the Curie-Weiss analysis gives a Weiss temperature $\Theta=-1.9 \pm 0.1$ K and an effective magnetic moment $\mu_{eff}=3.3 \pm 0.1 \mu_B$ per Yb ion, a substantial fraction of the value of $4.54 \mu_B$ expected for a free Yb^{3+} ion. The inset shows that $1/\chi$ deviates below the linear behavior at $T < 20$ K, but remains finite at the lowest temperature. We will argue below that the general lack of agreement between the measured susceptibility and a single Curie-Weiss expression results from significant CEF effects, yielding a highly temperature dependent effective moment in YbRh_2Pb .

We derived the basic ingredients for devising a crystal field scheme for YbRh_2Pb from heat capacity measurements. The temperature dependence of the heat capacity $C(T)$ measured in zero field and at temperatures as large as 70 K is shown in Fig. 4a. We have estimated the phonon contribution to the heat capacity C_{ph} using the Debye expression and find a Debye temperature $\theta_D=213 \pm 5$ K. C_{ph} is subtracted from $C(T)$ in Fig. 4a to isolate the remaining magnetic and electronic contributions to the heat capacity. The latter is expected to

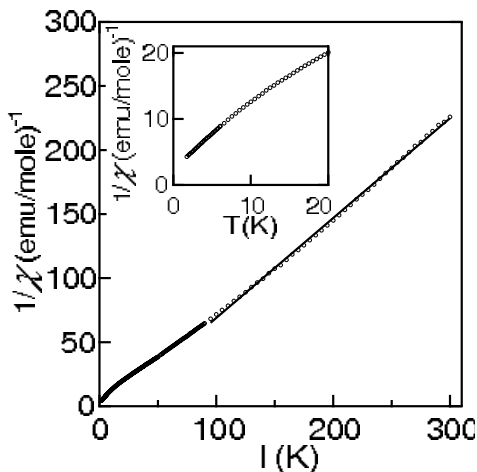


FIG. 3: Temperature dependence of the inverse of the magnetic susceptibility χ^{-1} of YbRh_2Pb measured in a field of 1000 Oe. Solid line is linear fit to $1/\chi = T/C - \Theta/C$ for temperatures between 100 K and 300 K, where C is the Curie constant and Θ is the Weiss temperature. The inset shows $1/\chi$ below $T=20$ K.

result in a component of the heat capacity which is linear in temperature, $C_{el} = \gamma T$. Accordingly we have plotted C/T as a function of T^2 in Fig. 4b, demonstrating that the electronic contribution can at best be identified over a very limited range of temperatures, yielding $\gamma = 4 \pm 1$ mJ/moleK². We conclude that the purely electronic contribution to the heat capacity is very small, as would be expected for weakly correlated conduction electrons or alternatively for a low density of conduction electrons for YbRh_2Pb . This implies, in turn, that $C - C_{ph}$ is largely magnetic. An expanded view of the temperature dependence of $C - C_{ph}$ is presented in Fig. 5, accompanied by the associated entropy S . The sudden increase in $C - C_{ph}$ near 0.57 K indicates a magnetic phase transition, possibly superposed on a broad Schottky peak. We have approximated $C - C_{ph}$ to zero temperature to account for the part of the heat capacity below 0.35 K inaccessible in our measurement. The entropy difference associated with the magnetic phase transition is only $0.78 \text{ Rln}2$, indicating that magnetic order does not develop from a well defined doublet ground state, alternatively an onset of the weak Kondo effect with the Kondo temperature $T_K < 0.5$ K can account for a reduced entropy. The entropy is roughly constant between 2 K and 10 K, subsequently increasing in proximity to a large Schottky anomaly centered at 28 K and approaching the full $\text{Rln}2$ only near 30 K.

Although the site symmetry of Yb in YbRh_2Pb is tetragonal and hence the CEF scheme must consist of 4 doublets, we show that the first excited doublet lies sufficiently close to the ground state doublet that the ground state can be considered a quartet. In Fig. 6 we schematically illustrate the CEF splitting scheme in YbRh_2Pb , which is derived from our heat capacity mea-

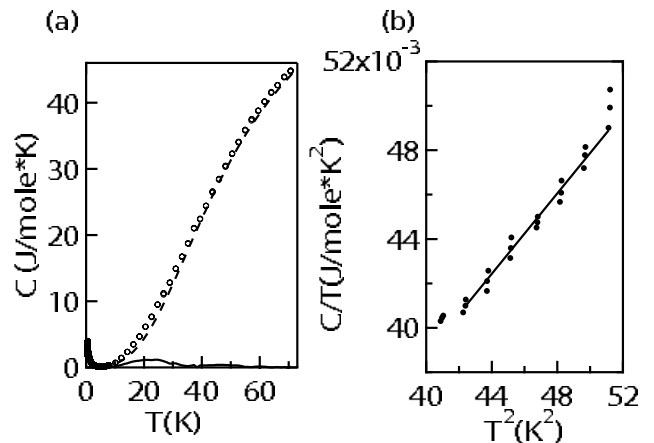


FIG. 4: (a) Temperature dependence of the heat capacity C (\circ) of YbRh_2Pb measured in zero field. The dashed line represents the Debye heat capacity, the solid line is the heat capacity with the lattice contribution subtracted. (b) The electronic part of the heat capacity $C_{el} = \gamma T$ is determined from this plot of $C/T = \gamma + \beta T^2$.

surements. The best fit to the broad maximum in the heat capacity at ~ 28 K (Fig. 5) was obtained assuming a fourfold degenerate ground state separated by an energy of $\Delta_1 = 68 \pm 5$ K from the first excited state, which is a doublet, and from the second excited state, also a doublet, by the energy $\Delta_2 = 300 \pm 60$ K. We conclude that the full Yb moment can only be regained at temperatures much higher than 300 K, and that at lower temperatures there is a substantially smaller and temperature dependent effective Yb moment.

To further test this CEF scheme we have measured $C(T)$ in a variety of fields between zero and 4 T. The data are presented in Fig. 7. Magnetic fields suppress the heat capacity jump at the magnetic transition. The ordering temperature also decreases in field, and Fig. 8 indicates that a magnetic field > 4 T is required to completely suppress magnetic order. For fields greater than ~ 2 T, the measured heat capacity mostly consists of a single broad peak which shifts to higher temperatures with increasing magnetic field. We attribute this peak to the Zeeman splitting of the ground state of YbRh_2Pb , which is a quartet in zero field. The field dependence of the heat capacity represented in Fig. 7 can be understood by assuming that the quartet is Zeeman split by the field into a ground state doublet and two excited singlets, as depicted in Fig. 6. Accordingly, in a field of 4 T, the heat capacity reaches ~ 2 J/mole \cdot K at $T_{max} = 0.448\Delta_z = 3.3$ K as expected for a system with a thermally activated occupation levels with degeneracy ratio of 0.5^{15} . The splitting Δ_z between the ground doublet and first excited doublet is deduced from Schottky fits to the data of Fig. 7, and Δ_z is itself plotted in Fig. 8. We note that including a second excited singlet state to this analysis did not significantly improve the quality of the fits. Δ_z increases approximately linearly to a value of 7 K in a field of 4

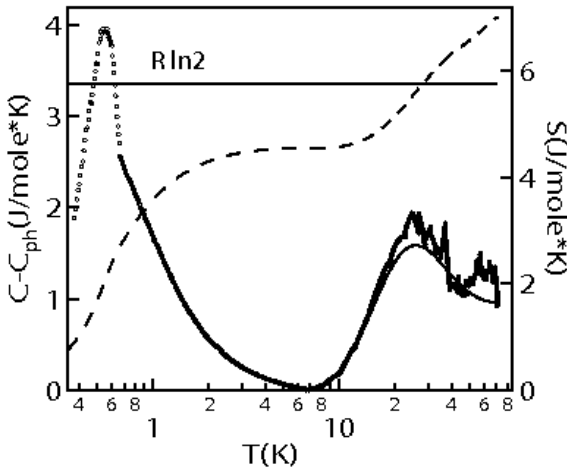


FIG. 5: Temperature dependence of the non-phonon heat capacity $C-C_{ph}$ (\circ) and the entropy S (dashed line) of YbRh_2Pb measured in zero field. The peak in $C-C_{ph}$ centered at 28 K is well fit by the Schottky expression described in the text (solid line).

T. Interestingly, Fig. 8 suggests that there is a residual splitting of ~ 1.5 K in zero field, which may perhaps account for the broad peak on which the magnetic anomaly is superposed (Fig. 5). Apart from this small splitting, the evolution of the heat capacity with magnetic fields indicates that the zero field ground state of YbRh_2Pb is fourfold degenerate. It would be interesting to further test this level scheme in YbRh_2Pb using inelastic neutron scattering experiments.

Given the magnitudes of the splittings in the CEF

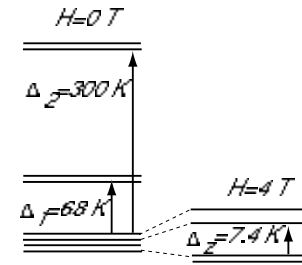


FIG. 6: Proposed zero field CEF scheme for Yb^{3+} in YbRh_2Pb (left). Application of a magnetic field lifts the degeneracy of the ground state quartet by an amount Δ_z , which is 7.4 K at 4 T (right).

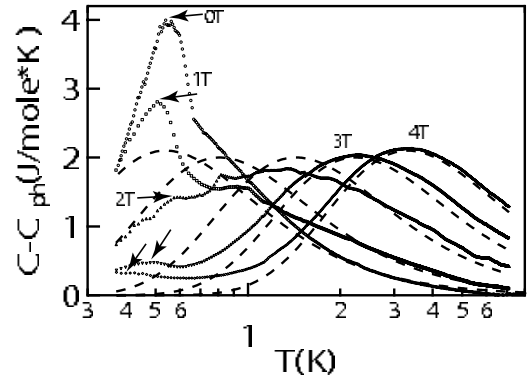


FIG. 7: Temperature dependence of the heat capacity of YbRh_2Pb measured in magnetic fields with the lattice contribution subtracted. Dashed lines represent the Schottky heat capacity C_{sch} of the two-level system, when the levels are split by the magnetic field.

scheme of YbRh_2Pb which are revealed by our analysis of the heat capacity, we expect that the effective Yb moment varies considerably over the temperature range 1.8 K - 300 K spanned by our measurements. As we have observed in our discussion of Fig. 3, this implies that χ cannot be fit by the Curie-Weiss law over an extensive range of temperatures. This is illustrated in the Fig. 9, where we plotted the effective magnetic moment $\mu_{eff}(T) = \sqrt{\frac{3k_B T \chi}{N}}$ as a function of temperature. With increased temperature, μ_{eff} increases as the excited states become occupied. However, the full Yb^{3+} Hund's rule moment of $4.54 \mu_B$ is not regained even at temperatures as large as 300 K.

The interplay between moment degeneracy and intermoment interactions strongly impacts the stability of magnetic order in YbRh_2Pb , which only occurs below 0.57 K. While neutron diffraction measurements would be required to unambiguously establish the type of magnetic order, the relatively weak field dependence of the transition temperature and the absence of appreciable broadening of the transition in the heat capacity suggest that YbRh_2Pb is an antiferromagnet. Magnetic order arises within a ground state quartet, which is further split into a doublet separated from the first of two excited

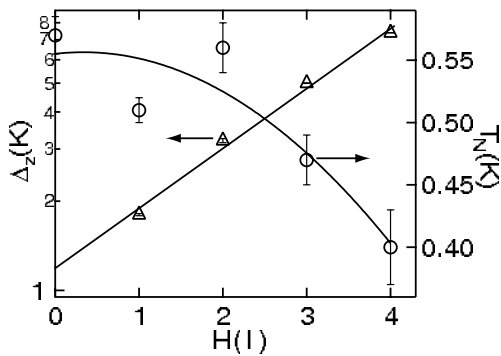


FIG. 8: Suppression of the magnetic ordering temperature T_N with increasing magnetic field (o); Δ indicates the Zee-man splitting Δ_z of the ground state quartet, taken from the Schottky analysis of the heat capacity described in the text. Solid lines are guides for the eye.

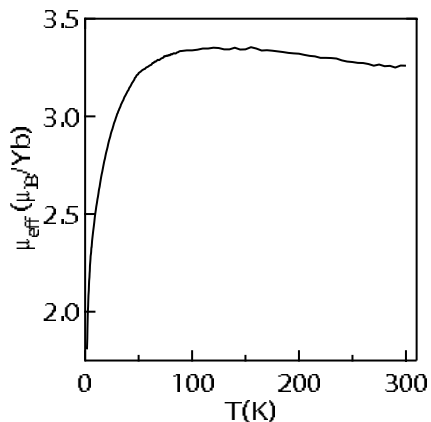


FIG. 9: The temperature dependent effective magnetic moment $\mu_{eff}(T) = \sqrt{\frac{3k_B T \chi}{N}}$ vs T.

singlets by ~ 1.5 K. Increasing this separation Δ_z with magnetic field results in the further suppression of the ordering temperature T_N . We observe that the successive actions of tetragonal and uniaxial CEF effects results in a paramagnetic state with a moment much reduced from the free ion value. At the same time, the small residual resistivity and the small electronic heat capacity suggest extremely weak hybridization between the Yb moment and the conduction electrons, and subsequently a small RKKY interaction among Yb moments. For these reasons, we believe that magnetic order in YbRh₂Pb is driven by a vanishingly small RKKY interaction acting on moments which have been reduced to a minimal value by CEF splittings which, while small in an absolute sense, are very large compared to T_N itself.

IV. CONCLUSION

We have synthesized the novel intermetallic Heusler compound YbRh₂Pb, which orders magnetically below $T_N=0.57$ K. The electrical resistivity displays an unusual linear temperature dependence, and its small residual value is consistent with good crystalline quality. Analyses of the heat capacity and the magnetic susceptibility indicate that the CEF splits the eight-fold degenerate ground state of Yb³⁺ into a ground state quartet and two excited doublets separated from the ground state by 68 K and 300 K, respectively. Magnetic fields further split the ground state, and we propose that this reduction in the effective moment is responsible for the observed reduction in the ordering temperature. Given the strong current interest in the quantum critical behavior which is found near phase transitions which occur at low or zero temperatures¹⁶, it is interesting to consider whether YbRh₂Pb belongs to this class of materials. While YbRh₂Pb orders at a very low temperature, one which can be reduced still further by applying a magnetic field, it is unlikely that quantum critical behavior will be observable in this system. The purely local moment nature of the magnetism, paired with the absence of correlation effects among the conduction electrons suggest that YbRh₂Pb belongs instead to the weak coupling limit of the Doniach phase diagram¹⁷. Without a large magnetic energy scale, the conventional critical phenomena associated with the small but finite temperature magnetic phase transition will limit any non-Fermi liquid behavior in YbRh₂Pb to very small reduced temperatures¹⁸.

V. ACKNOWLEDGMENTS

Work at the University of Michigan was performed under grant NSF-DMR-0405961. D. A. S. acknowledges useful conversations with Z. Fisk. The electron microprobe used in this study was partially funded by grant EAR-99-11352 from the National Science Foundation. Use of the National Synchrotron Light Source, Brookhaven National Laboratory, was supported by the U.S. Department of Energy, Office of Science, Office of Basic Energy Sciences, under Contract No. DE-AC02-98CH10886. We are grateful to Joseph Lauher for the use of X-ray diffraction facilities at the Stony Brook University Chemistry Department.

† e-mail address: sokolov@bnl.gov (D. A. Sokolov)

¹ P. J. Webster, *Contemp. Phys.* **10**, 559 (1969).

² M. Ishikawa, J-L. Jorda, and A. Junod, in *Superconductivity in d- and f-Band Metals*, edited by W. Buckel and W.

Weber (Kernforschungszentrum, Karlsruhe, 1982), p. 141.
³ S. K. Malik, A. M. Umarji, and G. K. Shenoy, *Phys. Rev. B.* **31**, 6971 (1985).

- ⁴ H. A. Kierstead, B. D. Dunlap, S. K. Malik, A. M. Umarji, and G. K. Shenoy, Phys. Rev. B. **32**, 135 (1985).
- ⁵ R. N. Shelton, L. S. Hausermann-Berg, M. J. Johnson, P. Klavins, and H. D. Yang, Phys. Rev. B. **34**, 199 (1986).
- ⁶ H. B. Stanley and J. W. Lynn, R. N. Shelton and P. Klavins, J. Appl. Phys. **61**, 3371 (1987).
- ⁷ W-H. Li, J. W. Lynn, and H. B. Stanley, T. J. Udovic, R. N. Shelton and P. Klavins, Phys. Rev. B. **39**, 4119 (1989).
- ⁸ C. L. Seaman, N. R. Dilley, M. C. de Andrade, J. Herrmann, M. B. Maple, and Z. Fisk, Phys. Rev. B. **53**, 2651 (1996).
- ⁹ Y. Aoki, H. R. Sato, H. Sugawara, H. Sato, Physica C. **333**, 187 (2000).
- ¹⁰ K. Gofryk, D. Kaczorowski, and T. Plackowski, A. Leithe-Jasper and Yu. Grin, Phys. Rev. B. **72**, 094409 (2005).
- ¹¹ J. C. Suits, Solid State Commun., **18**, 423 (1976).
- ¹² Topas V3: General Profile and Structure Analysis Software for Powder Diffraction Data; Bruker AXS, Karlsruhe, Germany. An academic version of Topas is available from <http://members.optusnet.com.au/~alancoelho>.
- ¹³ M. F. Gendron and R. E. Jones, J. Phys. Chem. Solids. **23**, 405 (1962).
- ¹⁴ see, for instance, L. Civale and E. N. Martinez, Phys. Rev. B **38**, 928 (1988) and the references therein.
- ¹⁵ J. G. Sereni, in *Handbook on the Physics and Chemistry of Rare Earths*, edited by K. A. Gschneidner, Jr. and L. Eyring (North-Holland, Amsterdam, 1991), p. 141.
- ¹⁶ G. R. Stewart, Rev. Mod. Phys. **73**, 797 (2001).
- ¹⁷ S. Doniach, Physica (Amsterdam) **91B + C**, 231 (1977).
- ¹⁸ A. J. Millis, Phys. Rev. B **48**, 7183 (1993).